

Vortex and half-vortex dynamics in a spinor quantum fluid of interacting polaritons

Lorenzo Dominici,^{1,2,*} Galbadrakh Dagvadorj,³ Jonathan M. Fellows,^{3,†} Stefano Donati,^{1,2}
Dario Ballarini,¹ Milena De Giorgi,¹ Francesca M. Marchetti,⁴ Bruno Piccirillo,⁵ Lorenzo
Marrucci,⁵ Alberto Bramati,⁶ Giuseppe Gigli,¹ Marzena H. Szymańska,⁷ and Daniele Sanvitto¹

¹ NANOTEC, Istituto di Nanotecnologia–CNR, Via Arnesano, 73100 Lecce, Italy

² Istituto Italiano di Tecnologia, IIT–Lecce, Via Barsanti, 73010 Lecce, Italy

³ Department of Physics, University of Warwick, Coventry CV47AL, UK

⁴ Departamento de Física Teórica de la Materia Condensada, UAM, Madrid 28049, Spain

⁵ Dipartimento di Fisica, Università Federico II di Napoli, 80126 Napoli, Italy

⁶ Laboratoire Kastler Brossel, UPMC-Paris 6, ENS et CNRS, 75005 Paris, France

⁷ Department of Physics and Astronomy, UCL, London WC1E6BT, UK

Spinorial or multi-component Bose-Einstein condensates may sustain fractional quanta of circulation, vorticant topological excitations with half integer windings of phase and polarization. Matter-light quantum fluids, such as microcavity polaritons, represent a unique test bed for realising strongly interacting and out-of-equilibrium condensates. The direct access to the phase of their wavefunction enables us to pursue the quest of whether half vortices—rather than full integer vortices—are the fundamental topological excitations of a spinor polariton fluid. Here, we are able to directly generate by resonant pulsed excitations, a polariton fluid carrying either the half or full vortex states as initial condition, and to follow their coherent evolution using ultrafast holography. Surprisingly we observe a rich phenomenology that shows a stable evolution of a phase singularity in a single component as well as in the full vortex state, spiraling, splitting and branching of the initial cores under different regimes and the proliferation of many vortex anti-vortex pairs in self generated circular ripples. This allows us to devise the interplay of nonlinearity and sample disorder in shaping the fluid and driving the phase singularities dynamics.

VORTICES and topological excitations play a crucial role in our understanding of the universe, recurring in the fields of subatomic particles, quantum fluids, condensed matter and nonlinear optics, being involved in fluid dynamics and phase transitions ranging up to the cosmologic scale¹. Spacetime could be analogue to a superfluid² and elementary particles the excitations of a medium called the quantum vacuum³; whatever this modern view will take strength or not, phase singularities (i.e., vortices) of a quantum fluid (e.g., of a superfluid) are point-like and quantized quasi-particles by excellence. Here we make use of a specific experimental “quantum interface”: polariton condensates⁴, which are bosonic hybrid light-matter particles consisting of strongly coupled excitons and photons. The ± 1 spin components of the excitons couple to different polarisation states of light

making the Bose-degenerate polariton gas a spinor condensate. The realisation of exciton polariton condensates in semiconductor microcavities^{5,6} has paved the way for a prolific series of studies into quantum hydrodynamics in two-dimensional systems^{7–13}. Microcavity polaritons are particularly advantageous systems for the study of topological excitations in interacting superfluids, thanks to the stronger nonlinearities and peculiar dispersive and dissipative features, with respect to both atomic condensates and nonlinear optics.

For the equilibrium spinor polariton fluid, in which the drive and decay processes are ignored, the lowest energy topological excitations have been predicted to be “half vortices” (HV)^{14,15}. These carry a phase singularity in only one circular polarisation, such that in the linear polarisation basis they have a half-integer winding number for both the phase and field-direction¹⁶. Such an excitation is complementary to a “full vortex” (FV), which instead has a singularity in each circular polarisation. Even in this simplified equilibrium scenario the question of either HVs or FVs are dynamically stable has led to some debate^{17–19} due to the presence of an inherent TE-TM splitting, which often arises in semiconductor microcavities and couples HVs with opposite spin.^{14,17}. The issue is even more complicated in a real polariton system, which is always subject to drive and dissipation, and is intrinsically out of equilibrium²⁰. Indeed, in the case of an incoherently pumped polariton superfluid, in contrast to the equilibrium predictions, it has been theoretically demonstrated²¹ that both FV and HV are dynamically stable in the absence of a symmetry breaking between the linear polarisation states, while in its presence only full vortex states are seen to be stable. On the experimental side, the recent work of Manni et al²² shows the splitting of a spontaneously formed linear polarised vortex state (FV) into two circularly polarised vortices (HVs) under non-resonant pulsed excitation. However, in this case, formation and motion/pinning of these vortices are caused by strong inhomogeneities and disorder in specific locations of the sample rather than by any fundamental process intrinsic to the fluid.

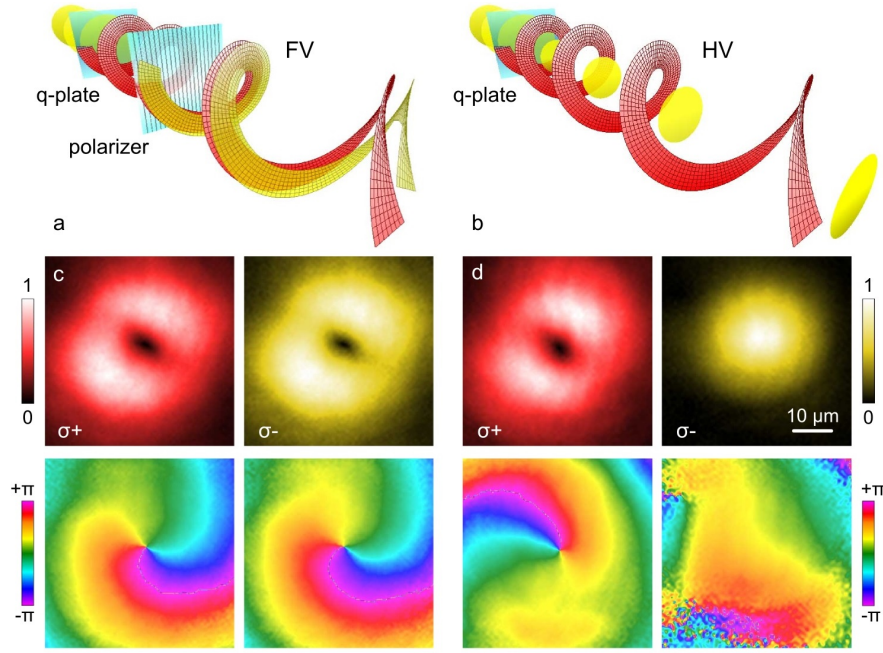


FIG. 1: Generation of optical and polariton FVs and HVs. (a,b) Experimental scheme for creation of optical full- (a) and half-vortex (b) state via a q-plate. The disks and helics represent the isophase surfaces for Gaussian and vortex beams, respectively, in the radial regions of larger intensity. Red and yellow colours refer to the σ_+ (σ_-) circular polarizations. (c,d) Emission density of the polariton fluid at the time of initial generation and the corresponding phase maps.

In general, the stability of vortex states in polariton condensates remains an open issue of fundamental importance, given that the nature of the elementary excitations is likely to affect the macroscopic properties of the system such as, for example, the conditions for the Berezinsky-Kosterlitz-Thouless (BKT) transitions to the superfluid state. On the application side, polariton vortices have been proposed also for ultra-sensitive gyroscopes²³ or information processing²⁴.

Experimental system

In this work we have been able for the first time to study the dynamics of half and full vortices created into a polariton condensate in a variety of initial conditions and in a controlled manner, taking advantage of the versatility of the resonant pumping scheme. We take care to generate the polariton vortex in a specific position on the sample with sufficiently weak disorder that the biasing effects of sample inhomogeneities can be screened out for a wide range of fluid densities.

In order to shape the phase profile of the incoming laser beam, we use a q-plate (Fig. 1), a patterned liquid crystal retarder recently developed to study laser windings and optical vorticity^{25–27}. The q-plate allows us, through appropriate optical and electrical tuning, to transform a Gaussian pulse into either a FV or a HV, according to the simplified schemes shown in Fig. 1 a,b. One advantage of a q-plate over using a typical SLM (space light modulator) is evident in the fact that the

latter device works for a given linear polarization, and two SLM are needed to create a HV. The exciting pulse is sent resonant on the microcavity sample to directly create a polariton fluid carrying either a full or half vortex, as shown from the emission maps in Fig. 1 c,d. Using a time-resolved digital holography^{28,29} technique for the detection, we measure both the instantaneous amplitude and phase of the polariton condensate³⁰ in all its polarization components. Each phase singularity can be digitally tracked so as to record the evolution of the resonantly created vortices after the initial pulse has gone but before the population has decayed away. The lifetime of the 2D polariton fluid in our microcavity sample^{31,32} kept at 10K is 10 ps, and we excite it by means of a 80 MHz train of 4 ps laser pulses resonant with the lower polariton energy at 836 nm.

Dynamics of half and full vortex

The creation of a HV is shown in Fig. 2 at different pulse powers. In panels (a,b) the trajectory of the primary vortex ($\Delta t: 5-15$ ps, $\delta t = 0.5$ ps) is superimposed to the amplitude map of the opposite spin (taken at $t = 15$ ps). For both powers, the singularity of the primary HV is seen moving along a circular trajectory around the density maximum of the opposing Gaussian state, keeping itself orbiting during few tenths of ps. Such curves are better depicted in Fig. 2 (c,d), which are the $(x(t), y(t), t)$ trajectories ($\Delta t: 5-40$ ps, $\delta t = 0.5$ ps) relative to cases (a,b), respectively, and in panel (e) reporting the angle θ and

distance d between the primary HV core and the Gaussian center of mass (see also Movie SM1).

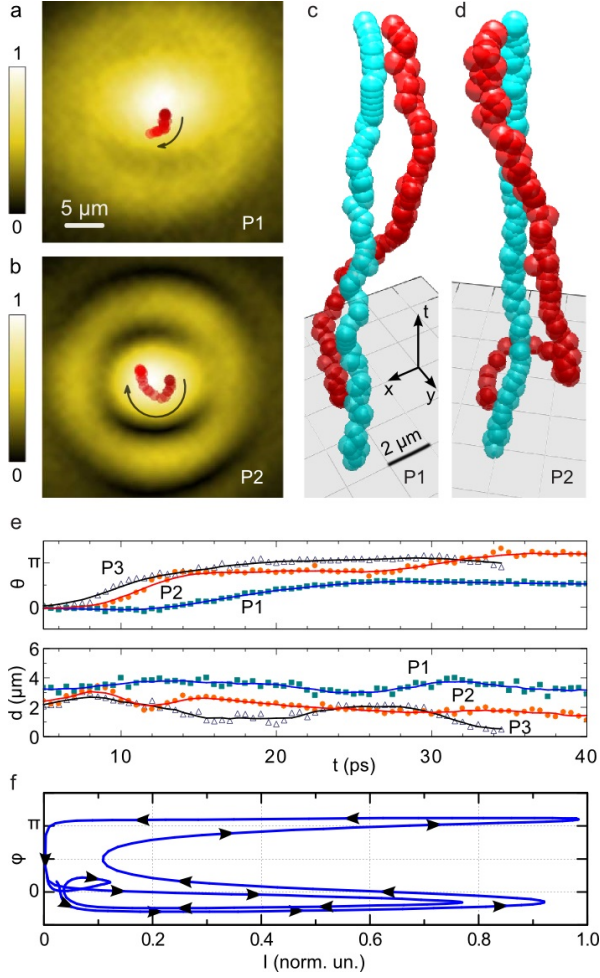


FIG. 2: Evolution of the main singularity upon HV injection. The Gaussian map is shown together with the core trajectory in the opposite σ , both 15 ps into the evolution, at the power of $P_1=0.77$ mW and $P_2=1.8$ mW in (a,b), respectively (see also Supporting Movie SM1 for power P_1). The complete (x, y, t) vortex trajectories (time range $\Delta t = 5 - 40$ ps, step $\delta t = 0.5$ ps) are shown in (c) and (d), with the blue spheres representing the Gaussian centroid and the red ones the phase singularity. The angle θ and distance d between the HV core and the opposite spin centroid are represented in (e) for 3 different powers. Panel (f) is the phase-intensity plot along a vertical cut for P_2 and $t=22$ ps (arrows follow y), highlighting a π -jump in the phase between adjacent maxima (i.e., when crossing the dark ring).

The orbital-like trajectories suggests the presence of interactions between the vortex of σ_+ polaritons and the opposite σ_- density. Such dynamical configuration resembles the metastable rotating vortex state, predicted in^{33,34}, supported by a harmonic trap, although this effective potential is dynamically modified by the intra-spin repulsive forces, e.g., by the deformation of the initial Gaussian. Indeed the nonlinearities induce a breaking of

radial symmetry, with the formation of circular ripples in the density. The dark ripple shown in Fig. 2 (b) relative to the σ_- Gaussian component, presents a π -jump in the phase ϕ , panel (f), which is a possible signature of a self-induced ring dark soliton (RDS), considered its nonlinear drive. It is known that RDS are possible solutions of a 2D fluid with repulsive interactions^{31,35,36}. Yet, the displacement of the singularity (density minimum) with respect to the centroid (opposite spin maximum), is consistent with attractive inter-spin forces. This is the first time that the manifestation of opposite spin interactions in polariton condensates is directly observed through their fluid dynamic effects.

In Fig. 3 we show the generation of a vortex with winding number $n = 1$ for each circular polarisation —i.e., a FV— that can then be detected separately. Panels (a-c) represent the amplitude maps of one population (σ_+) at $t=20$ ps with superposition of the vortices positions (trajectories for (a,b), instant positions for (c)) for three increasing pulse powers. The evolution of the primary singularities has been shown using 3D plots, i.e., $(x(t), y(t), t)$ curves, in the panels (d-f) corresponding to (a-c), respectively. In the linear regime, at which the polariton density is low (a,d, and Supporting Movie SM2), the opposite polarisation vortices evolve jointly for the first few picoseconds once the pulse has gone. As the density starts to drop, the vortex cores show an increasing separation in space, panel (g, orange), adopting independent trajectories. This suggests that the FV state is not intrinsically unstable, even though it may undergo splitting supposedly driven by the sample disorder; this is triggered when the density decreases below some critical value.

At larger polariton densities, Fig. 3 (b,e) and Movie SM3, at which the disorder is expected to be screened out, the twin singularities of the injected FV move together while the fluid is reshaped under the drive of the nonlinear interactions and the increase of radial flow. Here, they also undergo a spiraling similar to the HV case. Interestingly, the twin cores appear to follow the same initial path, see also panel (g, violet), hence indicating the lack of any intrinsic tendency of the FV state to split. This is confirmed by increasing the polariton density further, Fig. 3 (c,f) and (g, cyan), where the twin cores remain together for even longer times. Any potential instability of a FV, and the consequent tendency to split into two HV, is not observed here, differently from what observed in²², where the splitting after non-resonant pumping was due to marked sample inhomogeneities. On the contrary our results show that at high densities, for which the internal currents should prevail, there is a strong inclination for the system to keep the full vortex state together. However, note that the increased density eventually causes circular density ripples, which appear due to nonlinear radial currents and lead to the proliferation of vortex-antivortex (V-AV)

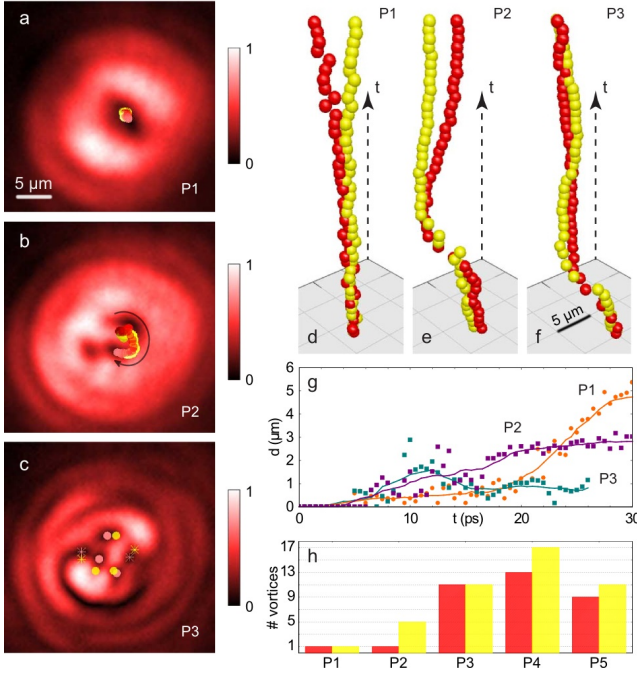


FIG. 3: Density maps and phase singularities upon resonant injection of FV states at different power regimes. (a-c) are the σ_+ density at $t = 20$ ps with superimposed phase singularities for both polarization, marked by symbols (circle for V, star for AV, colour for spin) (see Movies SM2–SM4). The trajectories of the primary vortices appear in (d-f) as 3D curves (x, y, t) (time range $\Delta t = 5 - 26$ ps, step $\delta t = 0.5$ ps) (see Movie SM5 for P_1), and the evolution of the inter-core distance is resumed in (g). The final panel (h) shows the proliferation of secondary pairs (at $t = 30$ ps) upon increasing pump power. The used laser powers are $P_{1-5} = 0.17, 0.77, 1.8, 3.1$ and 4.4 mW, which correspond to an initial excitation of $0.2, 1.0, 1.8, 2.2$ and $2.6 \cdot 10^6$ total polaritons, respectively.

pairs in both polarisations. In particular, secondary vortices nucleate in the low density regions of those circular ripples (Fig. 3 c,h), which additionally disrupt the original vortex core (see also Movie SM4).

Theoretical Modeling

In order to get a better understanding of the experimental vortex dynamics and interactions between the fundamental excitations, we have performed numerical simulations. The theoretical analysis performed by Rubo and collaborators in Ref.¹⁴ is based on the minimisation of the total energy for an equilibrium polariton condensate of infinite dimensions, i.e., where the density profile far from the vortex core is homogeneous. This analysis allows to establish a phase diagram for the stability/instability of different vortex excitations. In contrast, here, we study the dynamics of finite size FV and HV states and their stability during the dissipative and nonlinear evolution of interacting spinorial components, by dynamical sim-

ulations. We consider a generalised dissipative Gross-Pitaevskii equations for coupled two-component excitons $\phi_{\pm}(x, y, t)$ and microcavity photon $\psi_{\pm}(x, y, t)$ fields:

$$\begin{aligned} i\hbar \frac{\partial \phi_{\pm}}{\partial t} &= \left(-\frac{\hbar^2}{2m_{\phi}} \nabla^2 - i\frac{\hbar}{\tau_{\phi}} \right) \phi_{\pm} + \frac{\hbar\Omega_R}{2} \psi_{\pm} \\ &\quad + g|\phi_{\pm}|^2 \phi_{\pm} + \alpha|\phi_{\mp}|^2 \phi_{\pm} \\ i\hbar \frac{\partial \psi_{\pm}}{\partial t} &= \left(-\frac{\hbar^2}{2m_{\psi}} \nabla^2 - i\frac{\hbar}{\tau_{\psi}} \right) \psi_{\pm} + \frac{\hbar\Omega_R}{2} \phi_{\pm} \\ &\quad + D(x, y) \phi_{\pm} + \beta \left(\frac{\partial}{\partial x} \pm i \frac{\partial}{\partial y} \right)^2 \psi_{\mp} + F_{\pm} \end{aligned} \quad (1)$$

In order to reproduce the experimental conditions, we introduce a disorder term $D(x, y)$ for the photon field to match the inhomogeneities of the cavity mirror. The potential $D(x, y)$ is a Gaussian correlated potential with an amplitude of strength $50 \mu\text{eV}$ and a $1 \mu\text{m}$ correlation length. Since the effective mass of the excitons, m_{ϕ} , is 4-5 orders of magnitude greater than that of the microcavity photons, m_{ψ} , we may safely neglect the kinetic energy of the excitons. The parameters in Eq.(1) are fixed so that to reproduce the experimental conditions, with an exciton and photon lifetimes of $\tau_{\phi} = 1000$ ps and $\tau_{\psi} = 5$ ps, respectively, a Rabi splitting $\Omega_R = 5.4$ meV and the exciton-exciton interactions strength $g = 2 \mu\text{eV} \cdot \mu\text{m}^2$. We take the strength of the inter-spin exciton interaction to be an order of magnitude weaker than the intra-spin interaction³⁷, so that $\alpha = -0.1g$. The coupling between different polarisations is given by the inter-spin interaction α and by the TE-TM splitting term β . Following Hivet *et al*³⁸, we fix the ratio between the two effective masses $m_{\psi}^{\text{TE}}/m_{\psi}^{\text{TM}}$ to 0.95 in order to have an intermediate TE-TM splitting $\beta = \frac{\hbar^2}{4} \left(\frac{1}{m_{\psi}^{\text{TE}}} - \frac{1}{m_{\psi}^{\text{TM}}} \right) = 0.026 \times \frac{\hbar^2}{2m_{\psi}}$. The initial laser pulse is modelled as a pulsed Laguerre-Gauss F_{\pm} :

$$F_{\pm}(\mathbf{r}) = f_{\pm} r^{|n_{\pm}|} e^{-\frac{1}{2} \frac{r^2}{\sigma_r^2}} e^{in_{\pm} \theta} e^{-\frac{1}{2} \frac{(t-t_0)^2}{\sigma_t^2}} e^{i(\mathbf{k}_p \cdot \mathbf{r} - \omega_p t)}$$

where the winding number of the vortex component in the \pm polarisation is n_{\pm} . The strength, f , has been selected so as to replicate the observed total photon output. The σ_r and σ_t parameters were chosen in order to have space width and time duration (FWHM) of the pump $20 \mu\text{m}$ and 4 ps, respectively, in line with the experimental settings. The pump is slowly switched on into the simulation, reaching its maximum at $t_0 = 5.5$ ps and cut out completely after $5\sigma_t$ so as to avoid any unintended phase-locking. We follow the dynamics of both full and half vortices shined resonantly with the lower polariton dispersion at $\mathbf{k}_p = 0$ and $\omega_p = -1$.

Our simulations show that only in the presence of the disorder term the imprinted vortex excitations undergo an erratic movement, both in the half and full vortex configurations. In agreement with the experiments the splitting of the FV is observed in the simulations only in the presence of disorder. In Fig. 4 (a,b,c) we plot the

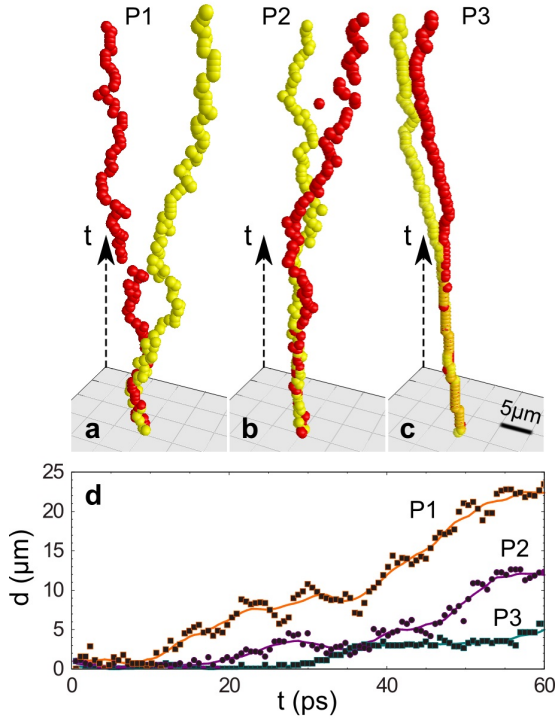


FIG. 4: Theoretical trajectories of primary singularities for FV state simulated at 3 increasing powers. (a-c) are the 3D (x, y, t) curves with $\delta t = 0.4$ ps step in a $\Delta t = 0 - 60$ ps span and the evolution of the inter-core distance is resumed in (d).

trajectories for different increasing powers P_{1-3} . The dissociation is seen at earlier times at low initial density, when the sample disorder potential is expected to play a pivotal role. At larger power the disorder and splitting are partially screened out, the main charges move jointly for a longer time. These results are resumed in the panel (d) and are in a good qualitative agreement with the experimental ones of Fig. 3. Simulations without disorder show that charges are dynamically stable, immune to any internal splitting. This holds in our simulations even with artificially enlarged α , confirming that any dissociation is an external rather than an intrinsic effect, at least during the polariton lifetime. In other terms, even though the thermodynamics would prefer HVs, based upon energy minimization¹⁴, the kinetics are too slow to observe such effect in a real system.

Branching and secondary vortices

In the experiments, as already stated, at large densities both the HV and FV develop concentric ripples, and this is causing generation of secondary vortices. For the HV, this effect is firstly seen by increasing the power in the initially vortex-free Gaussian component, where the same amount of total particles are concentrated in a smaller area than in the vortex counterpart. An exemplificative case of this regime is shown in Fig. 5, which reports

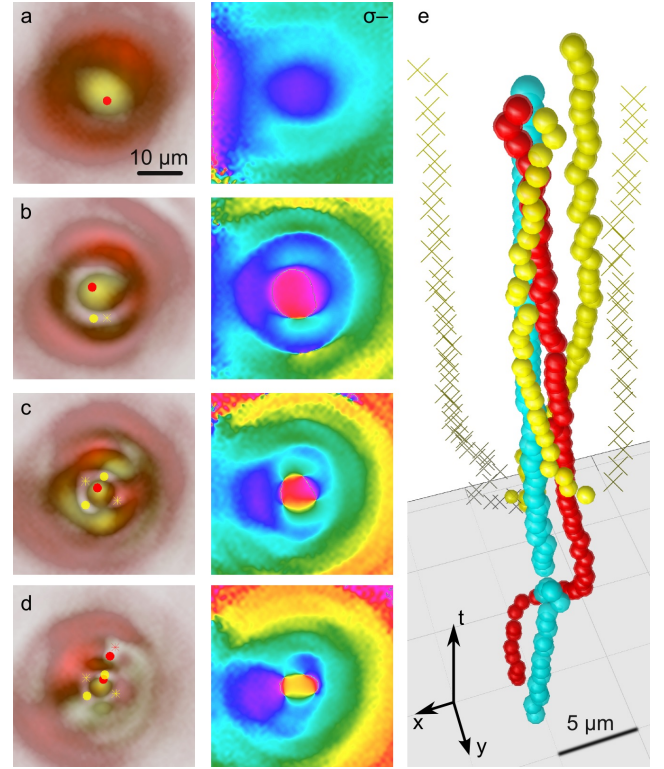


FIG. 5: Branching dynamics of a HV polariton condensate created at an intermediate power regime (1.8 mW). The four rows (a-d) show frames, taken at $t = 8, 16, 24$ and 32 ps, with densities and vortices in the first column and associated phase maps for σ_- in the second column. The initial condensate (a, orange due to overlap of red and yellow σ_{\pm} intensity scale) undergoes the formation of concentric ripples (b-d, see also Movie SM6). Spontaneous full V-AV formation with quadrupole symmetry for the initially Gaussian population is tracked and represented as (x, y, t) vortex strings with 0.5 ps time step in a $5 - 35$ ps time span (e, see Movie SM7).

in the first column the overlapped density maps of the two populations (red and yellow intensity scales) together with the vortices, and in the second column the σ_- phase maps. The condensate evolves from the initial time (a), where only the primary core of the HV is present, with the Gaussian developing more marked ripples, generating a first V-AV couple (b) and then a second one (c), which take positions in a 4-fold symmetric structure (see Movie SM6). This effect is not driven by disorder. It is intrinsic and observed in a very large number of realizations and in different polarizations. Generation of secondary V-AV pairs is also seen in simulations, where the disorder term is removed (see Fig 7), confirming that this effect is not caused by the sample disorder. The branching dynamics and its symmetry can be clearly seen also in the 3D (xyt) trajectories of panel (e) (see also Movie SM7). Only at later time (d), when the density decreases substantially, also the σ_+ component develops secondary pairs but in

an external region where the density drops locally. It is worth noting that at this later stage (d), the primary core of the HV, which was moving around, is seen to merge with a secondary vortex of the opposite polarization (but same winding), thus giving rise to the formation of a FV.

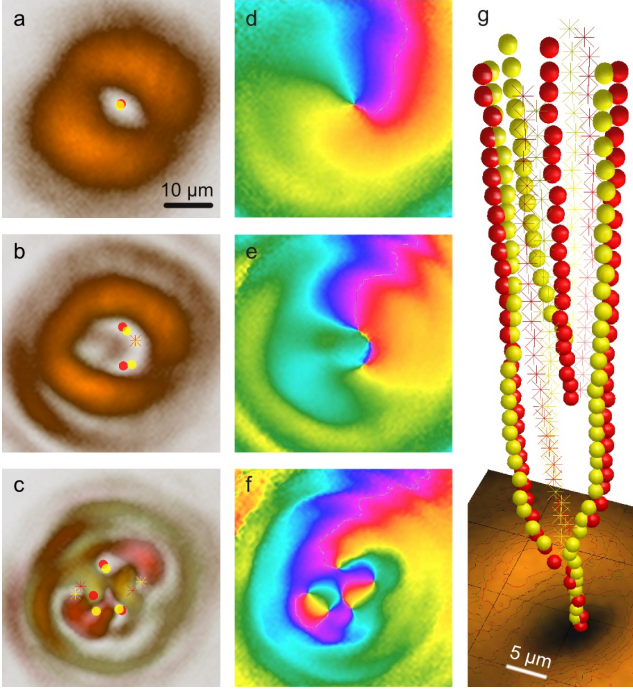


FIG. 6: Branching dynamics of a FV polariton condensate created at an intermediate power regime (1.8 mW). (a-c) are density frames and vortices taken at $t = 8, 12$ and 24 ps, respectively, while (d-f) are the corresponding phase maps for just one polarisation (σ_-). The initial condensate (a, orange due to overlap of red and yellow σ_{\pm}) develops concentric ripples (b-c, see also Movie SM4). Spontaneous full V-AV formation is tracked as (x, y, t) vortex branches with time step of $\delta t = 0.5$ ps and $\Delta t = 6 - 24$ ps range in (g, see Movie SM8), for both the populations. Each secondary HV stay close to its spin counterpart until quite late into the dynamics.

The generation of secondary vortices is seen also in case of the FV, as shown in Fig. 6, at $P = 1.8$ mW. The panels (a-c) represent the joint population and vortices at different time frames, while the corresponding phase maps (d-f) are reported only for one polarization. We observe that while the primary FV (a) rotates, it undergoes a displacement a moment before the creation of the first V-AV pair, which is followed by a second one, (b) and (c), respectively. The two secondary V-AV pairs are created in succession, and jointly between the two σ states: in other terms, the secondary topological charges are created as full vortex and anti-vortex. The σ_+ and σ_- cores of the primary and the first secondary FVs move together in a FV configuration for quite a long time. The branching and its partial symmetry, can be seen also in the phase maps (d-f), and in the branch structure of Fig. 6(g) (see

Movie SM8), with the xyt trajectories of the vortices. At later times the central region, initially dark, is partially filled with fluid and some degree of asymmetry is present between the two polariton distributions. We found that at different densities, localized transient structures with 3, 4 or 6-fold symmetries may arise too (see also²⁰).

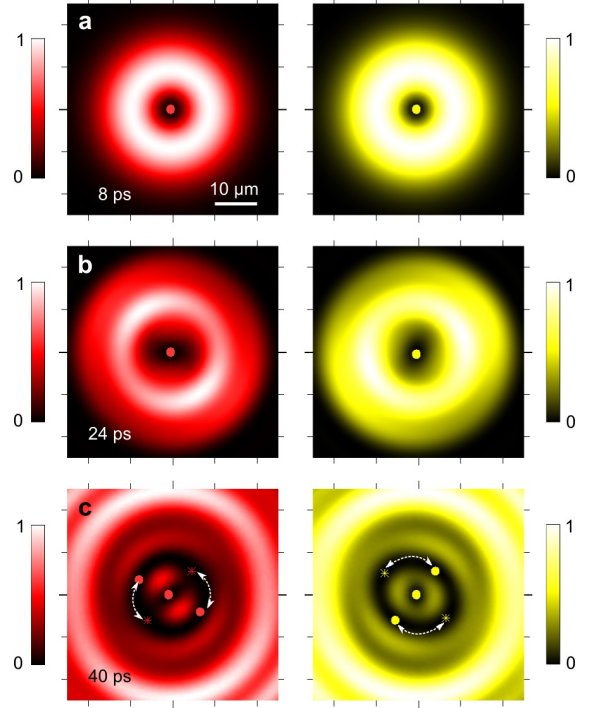


FIG. 7: Theoretical density maps and phase singularities in the case of FV without the disorder potential. (a-c) Each row corresponds to a different time, (a) $t = 8$ ps, (b) 24 ps and (c) 40 ps. Left and right columns represent the σ_+ and σ_- density, respectively, with superimposed their phase singularities, marked by symbols (circle for V, star for AV, colour for spin, see Movie SM9).

In the simulations we see the emergence of density ripples (radial symmetry breaking), as observed in the experiment, above certain density (pump power) threshold with or without the disorder. It is in the very bottom of these ripples, where the density is almost zero, that spontaneous V-AV pairs nucleate. Figure 7 shows the theoretical evolution of the density maps for the two components of a FV, on each column, respectively (see also Movie SM9). The main difference compared with experiments is that here the secondary couples are generated in different positions for the two polarisations. Yet, they keep rotating along a direction depending on their winding, and not on their spins. We have reasons to believe that the direction of circulation could be associated to the winding sign and the direction of the fluid reshaping (i.e., contracting or expanding), but the study of such aspect is well beyond the scope of the present work.

Conclusions

To conclude, we have investigated the dynamics and branching of half and full vortices resonantly injected in an out-of-equilibrium polariton quantum fluid. The dynamics of these topological defects is ruled by the interplay between the non-linearity and the disorder landscape. Our main conclusion is that, surprisingly, both FV and HV states are intrinsically dynamically stable, i.e., the topological charges in the two spin components do not split because of intrinsic energy considerations during the lifetime of the polaritons, nor the singularity of a half-vortex is seen to attract an opposite spin counterpart. The splitting effects, we observe, can be attributed to the fact that at low density (long time) the fluid streamlines are affected more by the sample landscape, with disorder guiding the displacement of the vortices, and eventually separating the cores when a symmetry breaking term such as anisotropic or TE-TM splitting is at action. At intermediate density regimes, when sample inhomogeneities are screened out and nonlinear turbulence is moderate, the charges stay together for longer times. It is at even larger densities, when the main charges stay together up to tens of ps, that they are also seen to move in a marked precessing trajectory, both for the HV and FV states. Here, the nonlinearities drive radial flows with the reshaping of the fluid into circular ripples of alternating high and low density regions, where secondary vortices nucleate. This nucleation is systematic and distinct from the proliferation of vortices at very low densities, which are pinned by disorder, as demonstrated by the theoretical simulations performed in an homogeneous landscape—the secondary charges nucleate in pairs of opposite winding in each of the two spin populations, and their evolution is seen as quasi-ordered branching of 3D (2D+t) singularity trees. Our observations suggest that quantum phase-singularities might be seen as an analogue of fundamental particles, whose features can span from quantized events such as pair creation and recombination to vortex strings. Moreover, with both topological states seemingly stable during the typical polariton lifetimes, an interesting question left to be addressed is which excitations are relevant for the Kosterlitz-Thouless-type transition in these systems.

Acknowledgments

We acknowledge Giovanni Lerario for fruitful discussions, R. Houdré for the growth of the microcavity sample and the project ERC POLAFLOW for financial support. MHS acknowledges support from EPSRC (EP/I028900/2 and EP/K003623/2). FMM acknowledges financial support from the Ministerio de Economía y Competitividad (MINECO), projects No. MAT2011-22997 and No. MAT2014-53119-C2-1-R.

Supplemental Information

Supporting Movies are available online at this URL .

* Electronic address: lorenzo.dominici@gmail.com

† Electronic address: j.fellows@warwick.ac.uk

- [1] Zurek, W. H. Cosmological experiments in superfluid helium? *Nature* **317**, 505–508 (1985). URL <http://dx.doi.org/10.1038/317505a0>.
- [2] Liberati, S. & Maccione, L. Astrophysical constraints on planck scale dissipative phenomena. *Phys. Rev. Lett.* **112**, 151301 (2014). URL <http://link.aps.org/doi/10.1103/PhysRevLett.112.151301>.
- [3] Volovik, G. E. *The Universe in a Helium Droplet* (Oxford University Press, 2003). URL <http://ukcatalogue.oup.com/product/9780198507826.do>.
- [4] Byrnes, T., Kim, N. Y. & Yamamoto, Y. Exciton-polariton condensates. *Nature Physics* **10**, 803–813 (2014). URL <http://dx.doi.org/10.1038/nphys3143>.
- [5] Kasprzak, J. *et al.* Bose-Einstein condensation of exciton polaritons. *Nature* **443**, 409–14 (2006). URL <http://dx.doi.org/10.1038/nature05131>.
- [6] Balili, R., Hartwell, V., Snoke, D., Pfeiffer, L. & West, K. Bose-einstein condensation of microcavity polaritons in a trap. *Science* **316**, 1007–1010 (2007). URL <http://www.sciencemag.org/content/316/5827/1007.abstract>.
- [7] Dreismann, A. *et al.* Coupled counterrotating polariton condensates in optically defined annular potentials. *Proceedings of the National Academy of Sciences* **111**, 8770–8775 (2014). URL <http://www.pnas.org/content/111/24/8770.abstract>.
- [8] Roumpos, G. *et al.* Power-law decay of the spatial correlation function in exciton-polariton condensates. *Proceedings of the National Academy of Sciences* **109**, 6467–6472 (2012). URL <http://www.pnas.org/content/109/17/6467.abstract>.
- [9] Amo, A. *et al.* Polariton superfluids reveal quantum hydrodynamic solitons. *Science (New York, N.Y.)* **332**, 1167–70 (2011). URL <http://www.sciencemag.org/content/332/6034/1167.full>.
- [10] Pigeon, S., Carusotto, I. & Ciuti, C. Hydrodynamic nucleation of vortices and solitons in a resonantly excited polariton superfluid. *Physical Review B* **83**, 144513 (2011). URL <http://link.aps.org/doi/10.1103/PhysRevB.83.144513>.
- [11] Sanvitto, D. *et al.* Persistent currents and quantized vortices in a polariton superfluid. *Nature Physics* **6**, 527–533 (2010). URL <http://www.nature.com/doi/10.1038/nphys1668>.
- [12] Amo, A. *et al.* Superfluidity of polaritons in semiconductor microcavities. *Nature Physics* **5**, 805–810 (2009). URL <http://www.nature.com/doi/10.1038/nphys1364>.
- [13] Lagoudakis, K. G. *et al.* Quantized vortices in an exciton-polariton condensate. *Nature Physics* **4**, 706–710 (2008). URL <http://www.nature.com/doi/10.1038/nphys1051>.
- [14] Toledo-Solano, M., Mora-Ramos, M. E., Figueroa, A. & Rubo, Y. G. Warping and interactions of vortices in exciton-polariton condensates. *Phys. Rev. B* **89**, 035308 (2014). URL <http://link.aps.org/doi/10.1103/PhysRevB.89.035308>.

- 1103/PhysRevB.89.035308.
- [15] Rubo, Y. Half vortices in exciton polariton condensates. *Physical Review Letters* **99**, 106401 (2007). URL <http://link.aps.org/doi/10.1103/PhysRevLett.99.106401>.
 - [16] Liu, G., Snoke, D. W., Daley, A., Pfeiffer, L. N. & West, K. A new type of half-quantum circulation in a macroscopic polariton spinor ring condensate. *Proceedings of the National Academy of Sciences* **112**, 2676–2681 (2015). URL <http://www.pnas.org/content/112/9/2676.abstract>.
 - [17] Flayac, H., Shelykh, I. A., Solnyshkov, D. D. & Malpuech, G. Topological stability of the half-vortices in spinor exciton-polariton condensates. *Physical Review B* **81**, 045318 (2010). URL <http://link.aps.org/doi/10.1103/PhysRevB.81.045318>.
 - [18] Toledo Solano, M. & Rubo, Y. G. Comment on topological stability of the half-vortices in spinor exciton-polariton condensates. *Physical Review B* **82**, 127301 (2010). URL <http://link.aps.org/doi/10.1103/PhysRevB.82.127301>.
 - [19] Flayac, H., Solnyshkov, D. D., Malpuech, G. & Shelykh, I. A. Reply to comment on topological stability of the half-vortices in spinor exciton-polariton condensates. *Physical Review B* **82**, 127302 (2010). URL <http://link.aps.org/doi/10.1103/PhysRevB.82.127302>.
 - [20] Keeling, J. & Berloff, N. Spontaneous rotating vortex lattices in a pumped decaying condensate. *Physical Review Letters* **100**, 250401 (2008). URL <http://link.aps.org/doi/10.1103/PhysRevLett.100.250401>.
 - [21] Borgh, M. O., Keeling, J. & Berloff, N. G. Spatial pattern formation and polarization dynamics of a nonequilibrium spinor polariton condensate. *Physical Review B* **81**, 235302 (2010). URL <http://link.aps.org/doi/10.1103/PhysRevB.81.235302>.
 - [22] Manni, F., Lagoudakis, K. & Liew, T. C. H. Dissociation dynamics of singly charged vortices into half-quantum vortex pairs. *Nature Communications* **3**, 1309 (2012). URL <http://www.nature.com/ncomms/journal/v3/n12/abs/ncomms2310.html>.
 - [23] Franchetti, G., Berloff, N. G. & Baumberg, J. J. Exploiting quantum coherence of polaritons for ultra sensitive detectors. *arXiv:1210.1187 [cond-mat.quant-gas]* (2012). URL <http://arxiv.org/abs/1210.1187>.
 - [24] Sigurdsson, H., Egorov, O. A., Ma, X., Shelykh, I. A. & Liew, T. C. H. Information processing with topologically protected vortex memories in exciton-polariton condensates. *Phys. Rev. B* **90**, 014504 (2014). URL <http://link.aps.org/doi/10.1103/PhysRevB.90.014504>.
 - [25] Marrucci, L., Manzo, C. & Paparo, D. Optical Spin-to-Orbital Angular Momentum Conversion in Inhomogeneous Anisotropic Media. *Physical Review Letters* **96**, 163905 (2006). URL <http://link.aps.org/doi/10.1103/PhysRevLett.96.163905>.
 - [26] D'Ambrosio, V. *et al.* Photonic polarization gears for ultra-sensitive angular measurements. *Nature Communications* **4**, 2432 (2013). URL <http://www.nature.com/ncomms/2013/130918/ncomms3432/abs/ncomms3432.html>.
 - [27] Cardano, F., Karimi, E., Marrucci, L., de Lisio, C. & Santamato, E. Generation and dynamics of optical beams with polarization singularities. *Optics Express* **21**, 8815–20 (2013). URL <http://www.opticsexpress.org/abstract.cfm?URI=oe-21-7-8815>.
 - [28] Antón, C. *et al.* Role of supercurrents on vortices formation in polariton condensates. *Optics Express* **20**, 16366 (2012). URL <http://www.opticsexpress.org/abstract.cfm?URI=oe-20-15-16366>.
 - [29] Nardin, G. *et al.* Selective photoexcitation of confined exciton-polariton vortices. *Physical Review B* **82**, 073303 (2010). URL <http://link.aps.org/doi/10.1103/PhysRevB.82.073303>.
 - [30] Dominici, L. *et al.* Ultrafast control and rabi oscillations of polaritons. *Phys. Rev. Lett.* **113**, 226401 (2014). URL <http://link.aps.org/doi/10.1103/PhysRevLett.113.226401>.
 - [31] Dominici, L. *et al.* Real-space collapse of a polariton condensate. *arXiv:1309.3083 [cond-mat.quant-gas]* (2013). URL <http://arxiv.org/abs/1309.3083>.
 - [32] Ballarini, D. *et al.* All-optical polariton transistor. *Nature Communications* **4**, 1778 (2013). URL <http://www.nature.com/ncomms/journal/v4/n4/full/ncomms2734.html>.
 - [33] Ostrovskaya, E. A., Abdullaev, J., Desyatnikov, A. S., Fraser, M. D. & Kivshar, Y. S. Dissipative solitons and vortices in polariton Bose-Einstein condensates. *Physical Review A* **86**, 013636 (2012). URL <http://link.aps.org/doi/10.1103/PhysRevA.86.013636>.
 - [34] Gautam, S. Dynamics of the corotating vortices in dipolar Bose-Einstein condensates in the presence of dissipation. *arXiv:1404.7087 [cond-mat.quant-gas]* (2014). URL <http://arxiv.org/abs/1404.7087>.
 - [35] Rodrigues, A. S. *et al.* From nodeless clouds and vortices to gray ring solitons and symmetry-broken states in two-dimensional polariton condensates. *Journal of Physics: Condensed Matter* **26**, 155801 (2014). URL <http://stacks.iop.org/0953-8984/26/i=15/a=155801>.
 - [36] Manni, F. *et al.* Spin-to-orbital angular momentum conversion in semiconductor microcavities. *Phys. Rev. B* **83**, 241307 (2011). URL <http://link.aps.org/doi/10.1103/PhysRevB.83.241307>.
 - [37] Ferrier, L. *et al.* Interactions in Confined Polariton Condensates. *Physical Review Letters* **106**, 126401 (2011). URL <http://link.aps.org/doi/10.1103/PhysRevLett.106.126401>.
 - [38] Hivet, R. *et al.* Half-solitons in a polariton quantum fluid behave like magnetic monopoles. *Nature Physics* **8**, 724–728 (2012). URL <http://www.nature.com/doifinder/10.1038/nphys2406>.